Title

Multimodal Voxel-Based Meta-Analysis of White Matter Abnormalities in Alzheimer's Disease

Journal

Journal of Alzheimer's Disease, 47(2)

ISSN

1387-2877

Authors

Yin, Rui-Hua
Tan, Lan
Liu, Yong
et al.

Publication Date

2015

DOI

10.3233/jad-150139

Peer reviewed

HHS Public Access

Author manuscript

J Alzheimers Dis. Author manuscript; available in PMC 2018 January 08.

Published in final edited form as:

J Alzheimers Dis. 2015 ; 47(2): 495–507. doi:10.3233/JAD-150139.

Multimodal Voxel-Based Meta-Analysis of White Matter Abnormalities in Alzheimer's Disease

Rui-Hua Yin[a], **Lan Tan**[a,b,c,*], **Yong Liu**[d], **Wen-Ying Wang**[a], **Hui-Fu Wang**[c], **Teng Jiang**[c], **Joaquim Radua**[e,f], **Yu Zhang**[g], **Junling Gao**[h], **Elisa Canu**[i], **Raffaella Migliaccio**[j,k], **Massimo Filippi**[i,l], **Maria Luisa Gorno-Tempini**[m], and **Jin-Tai Yu**[a,c,m,*]

[a]Department of Neurology, Qingdao Municipal Hospital, School of Medicine, Qingdao University, Qingdao, China

[b]College of Medicine and Pharmaceutics, Ocean University of China, Qingdao, China

[c]Department of Neurology, Qingdao Municipal Hospital, Nanjing Medical University, Qingdao, China

[d]Brainnetome Center, National Laboratory of Pattern Recognition, Institute of Automation, Chinese Academy of Sciences, Beijing, China

[e]Department of Psychosis Studies, Institute of Psychiatry, King's College London, London, UK

[f]Research Unit, FIDMAG – CIBERSAM, Sant Boi de Llobregat, Barcelona, Spain

[g]Center for Imaging of Neurodegenerative Diseases, Department of Veterans Affairs Medical Center, San Francisco, CA, USA

[h]Department of Medicine, LKS Faculty of Medicine, the University of Hong Kong, Hong Kong SAR

[i]Neuroimaging Research Unit, Institute of Experimental Neurology, Division of Neuroscience, San Raffaele Scientific Institute, Vita-Salute San Raffaele University, Via Olgettina, Milan, Italy

[j]INSERM, U1127, Institut du Cerveau et de la Moelle Epiniere (ICM), Hopital de la Pitie-Salpetriere, Paris, France

[k]Department of Neurology, Institut de la memoire et de la maladie d'Alzheimer, Hopital de la Pitie-Salpetriere, AP-HP, Paris, France

[l]Department of Neurology, Institute of Experimental Neurology, Division of Neuroscience, San Raffaele Scientific Institute, Vita-Salute San Raffaele University, Milan, Italy

[m]Memory and Aging Center, Department of Neurology, University of California at San Francisco, San Francisco, CA, USA

Abstract

[*]Correspondence to: Dr. Jin-Tai Yu, Department of Neurology, University of California, San Francisco, 675 Nelson Rising Lane, Suite 190, Box 1207, San Francisco, CA 94158, USA. yujintai@163.com or jintai.yu@ucsf.edu and Dr. Lan Tan MD, PhD, Department of Neurology, Qingdao Municipal Hospital, School of Medicine, Qingdao University, No.5 Donghai Middle Road, Qingdao, Shandong Province 266071, China. Tel.: +1 415 514 5745; Fax: +1 415 476 0679; dr.tanlan@163.com.

SUPPLEMENTARY MATERIAL

The supplementary material is available in the electronic version of this article: http://dx.doi.org/10.3233/JAD-150139.

An increasing number of MRI investigations suggest that patients with Alzheimer's disease (AD) show not only gray matter decreases but also white matter (WM) abnormalities, including WM volume (WMV) deficits and integrity disruption of WM pathways. In this study, we applied multimodal voxel-wise meta-analytical methods to study WMV and fractional anisotropy in AD. Fourteen studies including 723 participants (340 with AD and 383 controls) were involved. The meta-analysis was performed using effect size signed differential mapping. Significant WMV reductions were observed in bilateral inferior temporal gyrus, splenium of corpus callosum, right parahippocampal gyrus, and hippocampus. Decreased fractional anisotropy was identified mainly in left posterior limb of internal capsule, left anterior corona radiata, left thalamus, and left caudate nucleus. Significant decreases of both WMV and fractional anisotropy were found in left caudate nucleus, left superior corona radiata, and right inferior temporal gyrus. Most findings showed to be highly replicable in the jackknife sensitivity analyses. In conclusion, AD patients show widespread WM abnormalities mainly in bilateral structures related to advanced mental and nervous activities.

Keywords

Alzheimer's disease; diffusion tension imaging; fractional anisotropy; magnetic resonance imaging; voxel-based morphometry; white matter

INTRODUCTION

Alzheimer's disease (AD) is a neurodegenerative disorder characterized by progressive deterioration of cognitive function (especially the memory decline), changes in behavior, and the degraded ability to carry out daily activities [1]. Now it is the most common cause of dementia in the elderly, with the pathological features of widespread cortical changes, loss of neurons, and presence of senile plaques and neurofibrillary tangles that are found in the early course of AD [2].

Currently for clinical diagnosis of AD, neuroimaging examinations, such as positron emission tomography (PET) and magnetic resonance imaging (MRI), are widely used. Among numerous imaging examination methods, morphological MRI scans are generally used to detect gray matter (GM) abnormalities for the early diagnosis of AD, including atrophy of the whole brain, hippocampal formation, and entorhinal cortex, as well as expansion of the temporal horn in the lateral ventricles [3]. However, there are increasing MRI investigations suggesting that AD patients also present with white matter (WM) abnormalities including WM volume (WMV) deficits and disruption of the integrity of WM pathways [4–6]. Methodologically, voxel-based morphometry (VBM) is an automated technique widely used for quantitative measurements of WMV in separate regions. It uses T1-weighted images to perform voxel-wise statistical tests with the purpose of discovering subtle brain volume changes in association with neuropsychiatric disorders [7]. Additionally, diffusion tension imaging (DTI) is used to assess the microstructural integrity of WM, which is more potent to provide detailed information about the structural characteristics of WM tracts in the brain compared with conventional MRI methods [8, 9], and fractional anisotropy (FA), which reflects fiber density, axonal diameter, and myelination in WM, is

thought to be the best parameter to observe the brain WM fiber tract structure in order to assess the WM integrity.

A careful characterization of WM abnormalities in AD avails deeper insight into the explanation for clinical symptoms in terms of disturbances of brain networks and fiber connections rather than by damage to a specific subcortical structure. An early VBM study investigating the WMV deficits in the corpus callosum (CC) of AD subjects not only found that the callosal atrophy was most significant in the anterior splenium and isthmus (which are crucial callosal fiber tracts that interconnect the two cortical hemispheres) but also revealed a positive correlation between the degree of cognitive decline as assessed by the Mini-Mental State Examination (MMSE) and the volume of the anterior body of the CC [10]. A VBM meta-analysis determined that significant WMV reductions in AD patients were observed in the left parahippocampal gyrus extending to the temporal WM, the right temporal WM extending to the parahippocampal gyrus and the posterior CC, which are structures close to memory formations [11]. Moreover, DTI studies to date have detected decreased FA values in AD groups compared with controls mainly in the CC, cingulate, and uncinate fasciculus [12–14].

This meta-analysis was designed to provide a quantitative and consistent summary of studies investigating WMV and FA abnormalities in AD using effect-size signed differential mapping (ES-SDM, http://www.sdmproject.com/), a meta-analytical method superior to previous coordinates-based method such as activation likelihood estimator and signed differential mapping (SDM)[15]. We used novel multi modal meta-analytical methods for the combination of different imaging modalities in the same meta-analysis, thus potentially offering insights that are not apparent from any given imaging modality alone [16, 17].

METHODS

Literature search and eligibility criteria

Systematic and comprehensive searches of the PubMed, and EMBASE (from 1990 to August 2014) databases were performed using the keywords “Alzheimer’s disease” and (“voxel-based morphometry” or “voxel” or “VBM”), and (“white matter”, or “diffusion tensor imaging” or “DTI”). In addition, manual searches were conducted within review papers and reference sections of individual papers. A study was eligible for inclusion if it (1) reported a voxel-based comparison of WMV or FA between patients with AD and healthy controls (HC) subjects; (2) the diagnosis of probable AD was made according to the criteria of the National Institute of Neurological and Communicative Disorders and Stroke/ Alzheimer’s Disease and Related Disorders Association (NINCDS-ADRDA) [18]; (3) reported the coordinates of the peaks of the alterations in a stereotactic space in three coordinates (x, y, z), either the Montreal Neurological Institute (MNI) or the Talairach template; (4) used significance thresholds that were either corrected for multiple comparisons or uncorrected with spatial extent thresholds; (5) published in English. If the authors were the same or the characteristics of the subjects and data in two or more studies were similar, studies with the most integrated data were included. Exclusion criteria were: (1) studies from which peak coordinates could not be retrieved from the published article or after contacting the authors; (2) studies with fewer than nine subjects in either the AD group

or the HC group; (3) studies limiting their analyses to specific regions of interest (ROI); and (4) studies using tract-based spatial statistics (TBSS), because TBSS restricts the analysis to a FA-derived tract skeleton and thus cannot be combined with whole-brain WMV and FA studies [19].

Data extraction

The coordinates in each study were independently extracted by one of the investigators (R.H.Y.) and checked by another investigator (W.Y.W.) to minimize data entry errors. This study followed the Meta-analysis Of Observational Studies in Epidemiology (MOOSE) guidelines [20].

Statistical analysis

Regional WMV changes between the AD group and the HC group were meta-analyzed using ES-SDM software, which has specific WMV templates [21]. The main analyses were complemented with a systematic whole-brain voxel-based jackknife sensitivity analysis to test the replicability of the results, which is conducted by repeating the main statistical analysis but discarding one different study each time [22]. If a previously significant brain region remains significant in all or most of the combinations of studies it can be concluded that this result is highly replicable. Default kernel size (FWHM = 20 mm) and statistical thresholds ($p < 0.005$, peak SDM $z \geq 1$, cluster extent ≥10 voxels) were applied [15]. In addition, we conducted a meta-regressions of regional WMV and the MMSE score. The meta-analysis of regional FA was methodologically identical to that of regional WMV but the equivalent regression analyses could not be conducted in regional FA because of an insufficient number of studies. Finally, a multimodal meta-analysis of regional WMV and FA abnormalities was performed in order to detect those brain regions showing differences in both WMV and FA. The multimodal approach combines various imaging modalities in the same meta-analysis so that to detect those brain regions which are affected across two or more imaging modalities but not apparent from any given imaging modality alone. We followed the approach described in Radua et al. [16, 17], which aims to obtain the overlap between the abnormal regions in the WMV and FA accounting for noise in the meta-analytic *p*-values and not to detect correlations between WMV and FA nor to increase power.

RESULTS

Included studies and sample characteristics

Of 571 potential studies screened, 59 potentially met inclusion criteria. After the final filtration, a total of 14 studies [23–36] were included in the meta-analysis (see Fig. 1 for the specific reasons of exclusion). One of the studies [24] provided two clinical datasets (one of early onset AD (EOAD) and one of late onset AD (LOAD)), compared with different HC groups and another [25] studied WMV and FA in different groups. Therefore, 16 datasets (11 WMV and 5 FA) were ultimately included in the meta-analysis. All of these studies performed the data analysis according to the optimized VBM protocol [37] using different version of Statistical Parametric Mapping (SPM) software (http://www.fil.ion.ucl.ac.uk/spm/). The SPM software package has been designed for the analysis of brain imaging data sequences to instantiate the construction and assessment of spatially extended statistical

processes used to test hypotheses about functional imaging data. These studies included a total of 723 participants: 340 with AD and 383 controls. No relevant differences between patients and HC were found in terms of age, as the original studies were already well matched in this respect. Demographic and clinical characteristics and technique details of the studies are included in Tables 1 and 2.

Differences in regional WMV

Data for this analysis were obtained from all 11 WMV data sets including 260 patients with AD and 300 healthy controls. In patients with AD, significantly WMV reductions were mainly found in bilateral inferior temporal gyrus, splenium of CC, right parahippocampal gyrus, and right hippocampus (Table 3, Fig. 2, complete results in Supplementary Table 1). No WMV increases were detected. These findings were highly replicated in the jackknife analysis (Supplementary Table 2). In the meta-regression analysis, we made the following observations: samples with higher mean MMSE tend to appear decreased WMV in the bilateral parahippocampal gyrus and samples with lower mean MMSE showed decreased WMV in right hippocampus and splenium of CC. The reduction of WMV in left inferior temporal gyrus was independent of MMSE (Table 4).

Differences in regional FA

A group comparison of FA between AD patients and healthy controls was carried out in 5 data sets including 80 patients with AD and 83 healthy controls. Patients showed significantly decreased FA in left posterior limb of internal capsule (PLIC), left anterior corona radiata, left thalamus, and left caudate nucleus (Table 3 and Fig. 3). No increased FA was detected. Results were moderately replicated in the jackknife analysis (Supplementary Tables 1 and 2).

Multimodal analysis

The result of the multimodal analysis is showed in Table 3: decreased WMV and FA were found in left caudate nucleus, left superior corona radiate, right inferior temporal gyrus, and some other areas (right retrolenticular part of internal capsule, left posterior corona radiate, right caudate nucleus and right superior longitudinal fasciculus) (Fig. 4 and Supplementary Table 1).

DISCUSSION

The current study conducted a multimodal meta-analysis for WM abnormalities (including WMV and FA) between patients with AD and HC subjects. The main finding of the meta-analysis was acquired by the ES-SDM software and our results of decreased WMV revealed significant WM atrophy in bilateral inferior temporal gyrus, splenium of CC, right parahippocampal gyrus, and right hippocampus. And according to the jackknife sensitivity analysis, the results were robust and highly replicable. The hippocampus and parahippocampal gyrus are both sections of limbic system, which has been proved to be regularly involved in AD for decades [38]. The limbic system is closely linked to olfaction, emotions, drives, autonomic regulation, and memory. Both hippocampus and parahippocampal gyrus play central role in memory formation and hippocampus is one of

the first brain regions to suffer damage in AD or the prodromal stage, mild cognitive impairment [39, 40]. There was a study indicated the parahippocampal atrophy could also serve as an early biomarker of AD [41]. In addition, it seems that the right hippocampus formation is more significant than left side according to our results. The right hippocampus is related to the spatial memory while the left side plays an important role in verbal memory. But we cannot identify whether this difference between the bilateral hippocampus formation associated with the specific symptoms and further validation research is needed. The bilateral inferior temporal gyrus is traversed by uncinate fasciculus and the fornix terminalis, WM tracts involved in memory formation. The uncinate fasciculus is concerned with the verbal memory and immediate recall of word pairs by connecting the frontal lobe, the insula, and the rostral part of the temporal lobe [42]. The fornix connects with other key limbic structures and projects from the hippocampus to the anterior thalamic nuclei, mammillary bodies, striatum, and frontal cortex [43]. It is noteworthy that the hippocampus, parahippocampal gyrus, uncinate fasciculus, and fornix all participated in the Papez circuit, which was demonstrated to be linked to episodic memory problems in AD [44, 45]. The CC, which connects the hemispheres and plays key roles in the integration of perception and action [46], has been investigated as an independent region of interest to discover its relevance with AD [47–49] and in addition, the CC was found to have a positive correlation with response times in AD patients [50] and the research proved that interhemispheric coupling, in which CC play an critical role, may improve the brain's ability to meet processing demands for cognitive demand in AD. Particularly, the splenium of CC, which consists of fiber tracts connecting the temporal–parietal–occipital cortex, the superior parietal region, and the occipital lobe [46], was found to be affected by AD in several studies [28, 51, 52]. According to the meta-regression results, the MMSE scores (measurement of the severity of cognitive impairment) are associated with affected brain regions. Patients with more severe cognitive symptoms (lower MMSE) shows atrophy mainly in right hippocampus and splenium of CC while patients of less serious cognitive impairment (higher MMSE) are prone to decreased WMV in the bilateral parahippocampal gyrus. But these founding need to be interpreted cautiously because they were driven by only few studies. Moreover, the mean years of education differ in different studies and the education influences the MMSE score to a great extent.

A previous meta-analysis of DTI in AD revealed FA decreases in all regions except for parietal WM and internal capsule [12]. However in our meta-analysis, we found significant decreased FA in left PLIC, left anterior corona radiata, left thalamus, and left caudate nucleus. The different results might be caused by the methodological factors and the sample size. Moreover the previous meta-analysis excluded studies those assessed FA globally using VBM and included studies that used manual tracing, masking, or tractography to study a priori-defined ROI, which is the fundamental difference in research design. The internal capsule is the major route by which the cerebral cortex connects with the brainstem and spinal cord and contains both ascending and descending axons. Here, the significantly reduced FA found within PLIC (SDM z-value = −2.934, $p = 0.065 \times 10^{-4}$) and the thalamus (SDM z-value = −2.749, $p = 0.13 \times 10^{-4}$) indicated significant involvement of corticothalamic and thalamocortical radiations [35]. Moreover, the PLIC contains the pyramidal tracts, which implied its effect in somatic movement. It is possible that the

impairment of the PLIC, which reflected by the decreased FA, is bound up with the movement disturbance in AD. The corona radiata, as the most prominent projection fibers, radiates out from the cortex and come together in the brain stem, which continues ventrally as the internal capsule. Corona radiata is related to the motor pathway and speculative analysis so that the damage of the anterior corona radiata could be associated with both motor and cognitive dysfunction. Caudate, as part of the basal ganglia, plays a vital functional role in forming new associations to acquire explicit memories, and in motor learning, which is also associated with both motor and cognitive dysfunction in AD. But one thing to note is that our results of the jackknife sensitivity analysis were not very significant (Supplementary Table 2) and this might be mainly attributed to the small number of the included studies of FA. Additionally, the results of the five included studies are quite distinct and with little overlap.

WMV and FA can both decrease in areas where fiber tracts are organized in parallel. In microcosm perspective, the decrease of volume (less amount of WM) and FA (water more free to flow in other directions) might be the result of a decrease of the number or diameter of the axons. But we cannot rule out other interpretations such as changes in membrane permeability or in the presence of non-axonal components (cells, vessels, or interstitial fluid). In the current multimodal analysis, the most significant regions include left caudate nucleus, left superior corona radiata, and right inferior temporal gyrus. As mentioned above, these structures were all significant in the separate WMV and FA analysis. But we also detected some areas which were less significant (Fig. 4) and among them the superior longitudinal fasciculus (SLF) is noteworthy. As the SLF arises from the prefrontal cortex, along the route connects with the frontal, parietal, occipital and ends at temporal lobe, so that the SLF has extensive contact with cognitive function.

Currently, the mechanisms underlying WM abnormalities in AD have not yet been fully clarified. One theory proposes that GM degeneration would lead to WM atrophy through demyelination in efferent pathways and destroy the integrity of WM tracts by Wallerian degeneration [53, 54]. This statement is supported by the fact that WM abnormalities generally parallel the pattern of GM pathology, which first occurs in the hippocampus and entorhinal cortex [55]. Alternatively, the retrogenesis hypothesis posits that WM degeneration is the result of myelin breakdown that occurs following a pattern reverse of myelogenesis, which means late-myelinated WM fibers (such as inferior longitudinal fasciculus and SLF) are more vulnerable than the early-myelinating WM fibers [14, 56]. But as we discussed above, the PLIC, as one typical early-myelinating WM fiber, showed significant decreased FA. Another argument is that AD-related pathological WM changes are caused by microvascular ischemic events or other myelin-related defects and contribute to cortical GM degeneration [57]. However, our meta-analysis do not aimed to verify the mechanisms of WM abnormalities and results should be interpreted with caution.

Moreover, studies assessing AD patients at different ages of onset also found the underlying explanations for WM lesions in EOAD and LOAD make some difference. Topographically, WM lesions in LOAD were more inclined to follow the anatomical distribution of GM atrophy [6], while the EOAD WM abnormalities showed a more distributed pattern involving the inter-hemispheric connections, limbic network, and major associative tracts

[4]. On one hand, some postmortem studies reported higher burdens of Aβplaques and neurofibrillary tangles in patients with EOAD [58, 59] to indicate that the greater microstructural WM abnormalities might be a distinctive distribution of early upstream events (such as Aβ deposition). On the other hand, another study, which showed no global and regional differences in Aβ burden between EOAD and LOAD, proposed that severe downstream neurodegenerative processes (including tau pathology) may play a central role in the pathogenesis of EOAD [60].

There are also many studies investigating WM abnormalities in other forms of neurodegeneration, such as frontotemporal dementia (FTD). It was reported that FTD targets the orbitofrontal network [61], while AD targets the posterior temporal hetero-modal network [62]. Moreover, a study compared the AD and FTD found greater reductions of FA in frontal brain regions in FTD than AD patients to indicate that the WM degradation seems to be more prominent in FTD than in AD [36].

The superiority of the current study is the use of a multimodal approach, which provides a unique multimodal view of WM alterations in AD. And to our knowledge, this is the first VBM meta-analysis of FA in AD patients. However, there are also several limitations in our study. First, the meta-analysis was conducted based on pooling stereotactic coordinates with significant differences rather than on raw data from the original studies and this leads to less accurate results. Second, there was some potential methodological heterogeneity, such as different preprocessing protocols (traditional or optimized), smoothing kernels, the use of different MRI machines and statistical thresholding methods. For instance, some studies used corrected *p*-values, whereas others did not. This could affect the precision of the estimation of the effect sizes [19]. Finally, we could not include TBSS studies [63–65] so that we were only able to roughly localize regions of potential abnormality, but could not distinguish the particular abnormal tract or tracts crossing these regions.

In summary, our results suggest that patients with AD have widespread WM abnormalities (both WMV deficits and disruption of the integrity of WM pathways). The prominent regions we detected follow the anatomical pattern of GM atrophy and most of them are relevant to cognitive function. But the precise mechanisms of the WM abnormalities and the potential effects of medication on WM in AD require further investigation.

Supplementary Material

Refer to Web version on PubMed Central for supplementary material.

Acknowledgments

This work was supported by grants from the National Natural Science Foundation of China (81471309, 81171209, 61422204), Qingdao Key Health Discipline Development Fund, Qingdao Outstanding Health Professional Development Fund, and Shandong Provincial Collaborative Innovation Center for Neurodegenerative Disorders.

Authors' disclosures available online (http://j-alz.com/manuscript-disclosures/15-0139r1).

References

1. Nussbaum RL, Ellis CE. Alzheimer's disease and Parkinson's disease. N Engl J Med. 2003; 348:1356–1364. [PubMed: 12672864]
2. Braak H, Braak E. Staging of Alzheimer's disease-related neurofibrillary changes. Neurobiol Aging. 1995; 16:271–278. discussion 278–284. [PubMed: 7566337]
3. Dickerson BC, Sperling RA. Neuroimaging biomarkers for clinical trials of disease-modifying therapies in Alzheimer's disease. NeuroRx. 2005; 2:348–360. [PubMed: 15897955]
4. Canu E, Agosta F, Spinelli EG, Magnani G, Marcone A, Scola E, Falautano M, Comi G, Falini A, Filippi M. White matter microstructural damage in Alzheimer's disease at different ages of onset. Neurobiol Aging. 2013; 34:2331–2340. [PubMed: 23623599]
5. Cash DM, Ridgway GR, Liang Y, Ryan NS, Kinnunen KM, Yeatman T, Malone IB, Benzinger TL, Jack CR Jr, Thompson PM, Ghetti BF, Saykin AJ, Masters CL, Ringman JM, Salloway SP, Schofield PR, Sperling RA, Cairns NJ, Marcus DS, Xiong C, Bateman RJ, Morris JC, Rossor MN, Ourselin S, Fox NC. Dominantly Inherited Alzheimer N. The pattern of atrophy in familial Alzheimer disease: Volumetric MRI results from the DIAN study. Neurology. 2013; 81:1425–1433. [PubMed: 24049139]
6. Agosta F, Pievani M, Sala S, Geroldi C, Galluzzi S, Frisoni GB, Filippi M. White matter damage in Alzheimer disease and its relationship to gray matter atrophy. Radiology. 2011; 258:853–863. [PubMed: 21177393]
7. Busatto GF, Diniz BS, Zanetti MV. Voxel-based morphometry in Alzheimer's disease. Expert Rev Neurother. 2008; 8:1691–1702. [PubMed: 18986240]
8. Gold BT, Powell DK, Andersen AH, Smith CD. Alterations in multiple measures of white matter integrity in normal women at high risk for Alzheimer's disease. Neuroimage. 2010; 52:1487–1494. [PubMed: 20493952]
9. Masutani Y, Aoki S, Abe O, Hayashi N, Otomo K. MR diffusion tensor imaging: Recent advance and new techniques for diffusion tensor visualization. Eur J Radiol. 2003; 46:53–66. [PubMed: 12648802]
10. Chaim TM, Duran FL, Uchida RR, Perico CA, de Castro CC, Busatto GF. Volumetric reduction of the corpus callosum in Alzheimer's disease *in vivo* as assessed with voxel-based morphometry. Psychiatry Res. 2007; 154:59–68. [PubMed: 17174533]
11. Li J, Pan P, Huang R, Shang H. A meta-analysis of voxel-based morphometry studies of white matter volume alterations in Alzheimer's disease. Neurosci Biobehav Rev. 2012; 36:757–763. [PubMed: 22192882]
12. Sexton CE, Kalu UG, Filippini N, Mackay CE, Ebmeier KP. A meta-analysis of diffusion tensor imaging in mild cognitive impairment and Alzheimer's disease. Neurobiol Aging. 2011; 32:2322e2325–2318.
13. Alves GS, O'Dwyer L, Jurcoane A, Oertel-Knochel V, Knochel C, Prvulovic D, Sudo F, Alves CE, Valente L, Moreira D, Fubetaer F, Karakaya T, Pantel J, Engelhardt E, Laks J. Different patterns of white matter degeneration using multiple diffusion indices and volumetric data in mild cognitive impairment and Alzheimer patients. PLoS One. 2012; 7:e52859. [PubMed: 23300797]
14. Stricker NH, Schweinsburg BC, Delano-Wood L, Wierenga CE, Bangen KJ, Haaland KY, Frank LR, Salmon DP, Bondi MW. Decreased white matter integrity in late-myelinating fiber pathways in Alzheimer's disease supports retrogenesis. Neuroimage. 2009; 45:10–16. [PubMed: 19100839]
15. Radua J, Mataix-Cols D, Phillips ML, El-Hage W, Kronhaus DM, Cardoner N, Surguladze S. A new meta-analytic method for neuroimaging studies that combines reported peak coordinates and statistical parametric maps. Eur Psychiatry. 2012; 27:605–611. [PubMed: 21658917]
16. Radua J, Romeo M, Mataix-Cols D, Fusar-Poli P. A general approach for combining voxel-based meta-analyses conducted in different neuroimaging modalities. Curr Med Chem. 2013; 20:462–466. [PubMed: 23157638]
17. Radua J, Borgwardt S, Crescini A, Mataix-Cols D, Meyer-Lindenberg A, McGuire PK, Fusar-Poli P. Multimodal meta-analysis of structural and functional brain changes in first episode psychosis and the effects of antipsychotic medication. Neurosci Biobehav Rev. 2012; 36:2325–2333. [PubMed: 22910680]

18. McKhann G, Drachman D, Folstein M, Katzman R, Price D, Stadlan EM. Clinical diagnosis of Alzheimer's disease: Report of the NINCDS-ADRDA Work Group under the auspices of Department of Health and Human Services Task Force on Alzheimer's Disease. Neurology. 1984; 34:939–944. [PubMed: 6610841]
19. Radua J, Grau M, van den Heuvel OA, Thiebaut de Schotten M, Stein DJ, Canales-Rodriguez EJ, Catani M, Mataix-Cols D. Multimodal voxel-based meta-analysis of white matter abnormalities in obsessive-compulsive disorder. Neuropsychopharmacology. 2014; 39:1547–1557. [PubMed: 24407265]
20. Stroup DF, Berlin JA, Morton SC, Olkin I, Williamson GD, Rennie D, Moher D, Becker BJ, Sipe TA, Thacker SB. Meta-analysis of observational studies in epidemiology: A proposal for reporting. Meta-analysis Of Observational Studies in Epidemiology (MOOSE) group. JAMA. 2000; 283:2008–2012. [PubMed: 10789670]
21. Radua J, Via E, Catani M, Mataix-Cols D. Voxel-based meta-analysis of regional white-matter volume differences in autism spectrum disorder versus healthy controls. Psychol Med. 2011; 41:1539–1550. [PubMed: 21078227]
22. Radua J, Mataix-Cols D. Voxel-wise meta-analysis of grey matter changes in obsessive–compulsive disorder. Br J Psychiatry. 2009; 195:393–402. [PubMed: 19880927]
23. Baxter LC, Sparks DL, Johnson SC, Lenoski B, Lopez JE, Connor DJ, Sabbagh MN. Relationship of cognitive measures and gray and white matter in Alzheimer's disease. J Alzheimers Dis. 2006; 9:253–260. [PubMed: 16914835]
24. Canu E, Frisoni GB, Agosta F, Pievani M, Bonetti M, Filippi M. Early and late onset Alzheimer's disease patients have distinct patterns of white matter damage. Neurobiol Aging. 2012; 33:1023–1033. [PubMed: 21074899]
25. Canu E, McLaren DG, Fitzgerald ME, Bendlin BB, Zoccatelli G, Alessandrini F, Pizzini FB, Ricciardi GK, Beltramello A, Johnson SC, Frisoni GB. Mapping the structural brain changes in Alzheimer's disease: The independent contribution of two imaging modalities. J Alzheimers Dis. 2011; 26(Suppl 3):263–274.
26. Guo X, Wang Z, Li K, Li Z, Qi Z, Jin Z, Yao L, Chen K. Voxel-based assessment of gray and white matter volumes in Alzheimer's disease. Neurosci Lett. 2010; 468:146–150. [PubMed: 19879920]
27. Honea RA, Thomas GP, Harsha A, Anderson HS, Donnelly JE, Brooks WM, Burns JM. Cardiorespiratory fitness and preserved medial temporal lobe volume in Alzheimer disease. Alzheimer Dis Assoc Disord. 2009; 23:188–197. [PubMed: 19812458]
28. Li S, Pu F, Shi F, Xie S, Wang Y, Jiang T. Regional white matter decreases in Alzheimer's disease using optimized voxel-based morphometry. Acta Radiol. 2008; 49:84–90. [PubMed: 18210317]
29. Migliaccio R, Agosta F, Possin KL, Rabinovici GD, Miller BL, Gorno-Tempini ML. White matter atrophy in Alzheimer's disease variants. Alzheimers Dement. 2012; 8:S78–87. e71–72. [PubMed: 23021625]
30. Serra L, Cercignani M, Lenzi D, Perri R, Fadda L, Caltagirone C, Macaluso E, Bozzali M. Grey and white matter changes at different stages of Alzheimer's disease. J Alzheimers Dis. 2010; 19:147–159. [PubMed: 20061634]
31. Takahashi R, Ishii K, Miyamoto N, Yoshikawa T, Shimada K, Ohkawa S, Kakigi T, Yokoyama K. Measurement of gray and white matter atrophy in dementia with Lewy bodies using diffeomorphic anatomic registration through exponentiated lie algebra: A comparison with conventional voxel-based morphometry. AJNR Am J Neuroradiol. 2010; 31:1873–1878. [PubMed: 20634303]
32. Villain N, Desgranges B, Viader F, de la Sayette V, Mezenge F, Landeau B, Baron JC, Eustache F, Chetelat G. Relationships between hippocampal atrophy, white matter disruption, and gray matter hypometabolism in Alzheimer's disease. J Neurosci. 2008; 28:6174–6181. [PubMed: 18550759]
33. Gao J, Cheung RT, Lee TM, Chu LW, Chan YS, Mak HK, Zhang JX, Qiu D, Fung G, Cheung C. Possible retrogenesis observed with fiber tracking: An anteroposterior pattern of white matter disintegrity in normal aging and Alzheimer's disease. J Alzheimers Dis. 2011; 26:47–58. [PubMed: 21558648]
34. Medina D, DeToledo-Morrell L, Urresta F, Gabrieli JD, Moseley M, Fleischman D, Bennett DA, Leurgans S, Turner DA, Stebbins GT. White matter changes in mild cognitive impairment and AD: A diffusion tensor imaging study. Neurobiol Aging. 2006; 27:663–672. [PubMed: 16005548]

35. Rose SE, Janke AL, Chalk JB. Gray and white matter changes in Alzheimer's disease: A diffusion tensor imaging study. J Magn Reson Imaging. 2008; 27:20–26. [PubMed: 18050329]
36. Zhang Y, Schuff N, Du AT, Rosen HJ, Kramer JH, Gorno-Tempini ML, Miller BL, Weiner MW. White matter damage in frontotemporal dementia and Alzheimer's disease measured by diffusion MRI. Brain. 2009; 132:2579–2592. [PubMed: 19439421]
37. Good CD, Johnsrude IS, Ashburner J, Henson RN, Friston KJ, Frackowiak RS. A voxel-based morphometric study of ageing in 465 normal adult human brains. Neuroimage. 2001; 14:21–36. [PubMed: 11525331]
38. Hopper MW, Vogel FS. The limbic system in Alzheimer's disease. A neuropathologic investigation. Am J Pathol. 1976; 85:1–20. [PubMed: 135514]
39. Hampel H, Burger K, Teipel SJ, Bokde AL, Zetterberg H, Blennow K. Core candidate neurochemical and imaging biomarkers of Alzheimer's disease. Alzheimers Dement. 2008; 4:38–48. [PubMed: 18631949]
40. Hong YJ, Yoon B, Lim SC, Shim YS, Kim JY, Ahn KJ, Han IW, Yang DW. Microstructural changes in the hippocampus and posterior cingulate in mild cognitive impairment and Alzheimer's disease: A diffusion tensor imaging study. Neurol Sci. 2013; 34:1215–1221. [PubMed: 23109096]
41. Echávarri C, Aalten P, Uylings HBM, Jacobs HIL, Visser PJ, Gronenschild EHBM, Verhey FRJ, Burgmans S. Atrophy in the parahippocampal gyrus as an early biomarker of Alzheimer's disease. Brain Struct Funct. 2011; 215:265–271. [PubMed: 20957494]
42. Serra L, Cercignani M, Basile B, Spano B, Perri R, Fadda L, Marra C, Giubilei F, Caltagirone C, Bozzali M. White matter damage along the uncinate fasciculus contributes to cognitive decline in AD and DLB. Curr Alzheimer Res. 2012; 9:326–333. [PubMed: 22272613]
43. Racine AM, Adluru N, Alexander AL, Christian BT, Okonkwo OC, Oh J, Cleary CA, Birdsill A, Hillmer AT, Murali D, Barnhart TE, Gallagher CL, Carlsson CM, Rowley HA, Dowling NM, Asthana S, Sager MA, Bendlin BB, Johnson SC. Associations between white matter microstructure and amyloid burden in preclinical Alzheimer's disease: A multimodal imaging investigation. Neuroimage Clin. 2014; 4:604–614. [PubMed: 24936411]
44. Carter SF, Embleton KV, Anton-Rodriguez JM, Burns A, Ralph MA, Herholz K. Regional neuronal network failure and cognition in late-onset sporadic Alzheimer disease. AJNR Am J Neuroradiol. 2014; 35:S18–S30. [PubMed: 24578281]
45. Hornberger M, Wong S, Tan R, Irish M, Piguet O, Kril J, Hodges JR, Halliday G. *In vivo* and post-mortem memory circuit integrity in frontotemporal dementia and Alzheimer's disease. Brain. 2012; 135:3015–3025. [PubMed: 23012333]
46. Schulte T, Muller-Oehring EM. Contribution of callosal connections to the interhemispheric integration of visuomotor and cognitive processes. Neuropsychol Rev. 2010; 20:174–190. [PubMed: 20411431]
47. Zhu M, Wang X, Gao W, Shi C, Ge H, Shen H, Lin Z. Corpus callosum atrophy and cognitive decline in early Alzheimer's disease: Longitudinal MRI study. Dement Geriatr Cogn Disord. 2014; 37:214–222. [PubMed: 24193144]
48. Zhu M, Gao W, Wang X, Shi C, Lin Z. Progression of corpus callosum atrophy in early stage of Alzheimer's disease: MRI based study. Acad Radiol. 2012; 19:512–517. [PubMed: 22342652]
49. Frederiksen KS, Garde E, Skimminge A, Ryberg C, Rostrup E, Baare WF, Siebner HR, Hejl AM, Leffers AM, Waldemar G. Corpus callosum atrophy in patients with mild Alzheimer's disease. Neurodegener Dis. 2011; 8:476–482. [PubMed: 21659724]
50. Ansado J, Collins L, Joubert S, Fonov V, Monchi O, Brambati SM, Tomaiuolo F, Petrides M, Faure S, Joanette Y. Interhemispheric coupling improves the brain's ability to perform low cognitive demand tasks in Alzheimer's disease and high cognitive demand tasks in normal aging. Neuropsychology. 2013; 27:464–480. [PubMed: 23876119]
51. Wang PJ, Saykin AJ, Flashman LA, Wishart HA, Rabin LA, Santulli RB, McHugh TL, MacDonald JW, Mamourian AC. Regionally specific atrophy of the corpus callosum in AD, MCI and cognitive complaints. Neurobiol Aging. 2006; 27:1613–1617. [PubMed: 16271806]
52. Zhang Y, Schuff N, Jahng GH, Bayne W, Mori S, Schad L, Mueller S, Du AT, Kramer JH, Yaffe K, Chui H, Jagust WJ, Miller BL, Weiner MW. Diffusion tensor imaging of cingulum fibers in mild cognitive impairment and Alzheimer disease. Neurology. 2007; 68:13–19. [PubMed: 17200485]

53. Tomimoto H, Lin J-X, Matsuo A, Ihara M, Ohtani R, Shibata M, Miki Y, Shibasaki H. Different mechanisms of corpus callosum atrophy in Alzheimer's disease and vascular dementia. J Neurol. 2004; 251:398–406. [PubMed: 15083283]

54. Medina DA, Gaviria M. Diffusion tensor imaging investigations in Alzheimer's disease: The resurgence of white matter compromise in the cortical dysfunction of the aging brain. Neuropsychiatr Dis Treat. 2008; 4:737–742. [PubMed: 19043518]

55. Braak H, Braak E. Diagnostic criteria for neuropathologic assessment of Alzheimer's disease. Neurobiol Aging. 1997; 18:S85–S88. [PubMed: 9330992]

56. Brickman AM, Meier IB, Korgaonkar MS, Provenzano FA, Grieve SM, Siedlecki KL, Wasserman BT, Williams LM, Zimmerman ME. Testing the white matter retrogenesis hypothesis of cognitive aging. Neurobiol Aging. 2012; 33:1699–1715. [PubMed: 21783280]

57. Bartzokis G. Alzheimer's disease as homeostatic responses to age-related myelin breakdown. Neurobiol Aging. 2011; 32:1341–1371. [PubMed: 19775776]

58. Bigio EH, Hynan LS, Sontag E, Satumtira S, White CL. Synapse loss is greater in presenile than senile onset Alzheimer disease: Implications for the cognitive reserve hypothesis. Neuropathol Appl Neurobiol. 2002; 28:218–227. [PubMed: 12060346]

59. Marshall GA, Fairbanks LA, Tekin S, Vinters HV, Cummings JL. Early-onset Alzheimer's disease is associated with greater pathologic burden. J Geriatr Psychiatry Neurol. 2007; 20:29–33. [PubMed: 17341768]

60. Rabinovici GD, Furst AJ, Alkalay A, Racine CA, O'Neil JP, Janabi M, Baker SL, Agarwal N, Bonasera SJ, Mormino EC, Weiner MW, Gorno-Tempini ML, Rosen HJ, Miller BL, Jagust WJ. Increased metabolic vulnerability in early-onset Alzheimer's disease is not related to amyloid burden. Brain. 2010; 133:512–528. [PubMed: 20080878]

61. Seeley WW, Crawford RK, Zhou J, Miller BL, Greicius MD. Neurodegenerative diseases target large-scale human brain networks. Neuron. 2009; 62:42–52. [PubMed: 19376066]

62. Acosta-Cabronero J, Williams GB, Pengas G, Nestor PJ. Absolute diffusivities define the landscape of white matter degeneration in Alzheimer's disease. Brain. 2010; 133(Pt 2):529–539. [PubMed: 19914928]

63. Wang PN, Chou KH, Lirng JF, Lin KN, Chen WT, Lin CP. Multiple diffusivities define white matter degeneration in amnestic mild cognitive impairment and Alzheimer's disease. J Alzheimers Dis. 2012; 30:423–437. [PubMed: 22430530]

64. Bosch B, Arenaza-Urquijo EM, Rami L, Sala-Llonch R, Junque C, Sole-Padulles C, Pena-Gomez C, Bargallo N, Molinuevo JL, Bartres-Faz D. Multiple DTI index analysis in normal aging, amnestic MCI and AD. Relationship with neuropsychological performance. Neurobiol Aging. 2012; 33:61–74. [PubMed: 20371138]

65. Di Paola M, Di Iulio F, Cherubini A, Blundo C, Casini AR, Sancesario G, Passafiume D, Caltagirone C, Spalletta G. When, where, and how the corpus callosum changes in MCI and AD: A multimodal MRI study. Neurology. 2010; 74:1136–1142. [PubMed: 20368633]

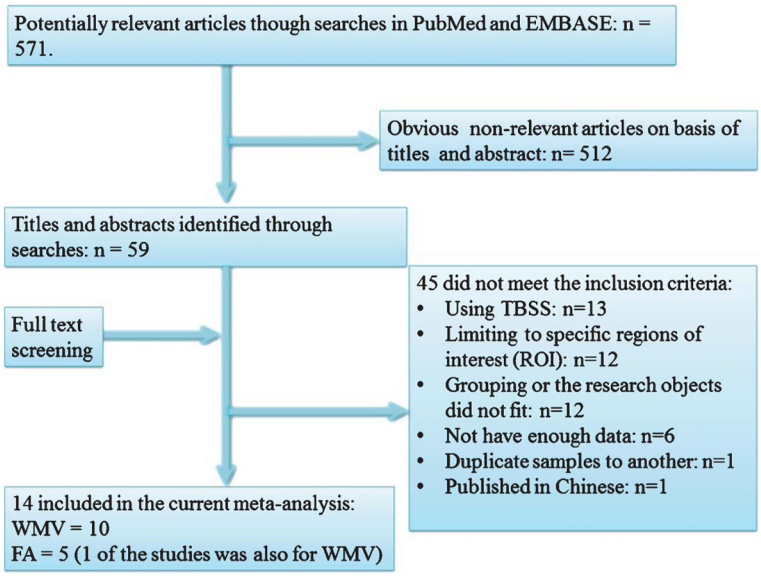

Fig. 1.

Identification and attrition of studies. Search terms were “Alzheimer’s disease” and (“voxel-based morphometry” or “voxel” or “VBM”), and (“white matter”, or “diffusion tensor imaging” or “DTI”). FA, fractional anisotropy; ROI, regions of interest; TBSS, tract-based spatial statistics; WMV, white matter volume.

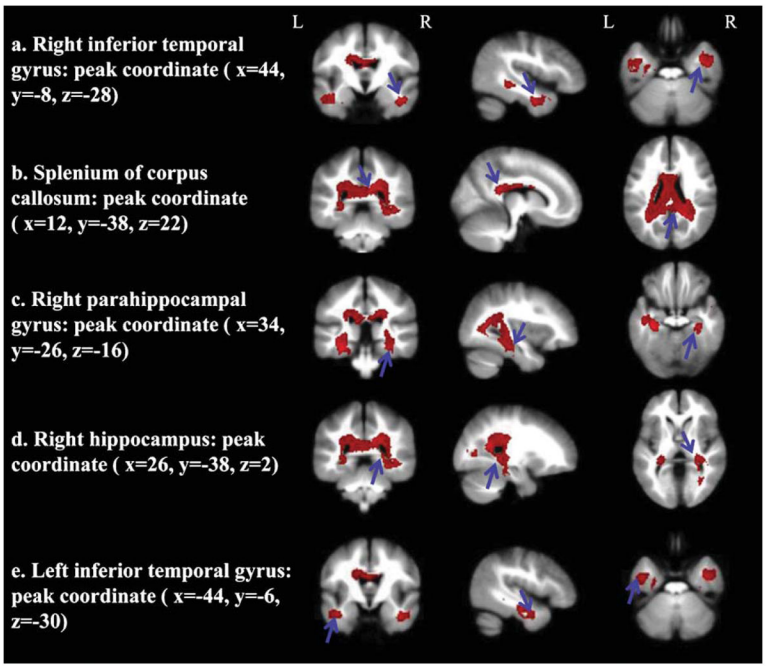

Fig. 2.

Regional WMV decreases in AD compared with HC. Only significant results ($p < 0.005$, correspond to SDM-Z ≤−1.976) and a cluster size >10 voxels are reported. Images are acquired in three planes (coronal, sagittal and axial sections) by MRIcron software which was binding with ES-SDM. The (a–e) successively indicate right inferior temporal gyrus, splenium of corpus callosum, right parahippocampal gyrus, right hippocampus, and left inferior temporal gyrus. The red color only represents the areas detected with WMV decreases and cannot signify the SDM z-value. The red area proportion shows the cluster size and the arrows indicate the specific point of the results. AD, Alzheimer's disease; HC, healthy control; L, left; R, right; WMV, white matter volume.

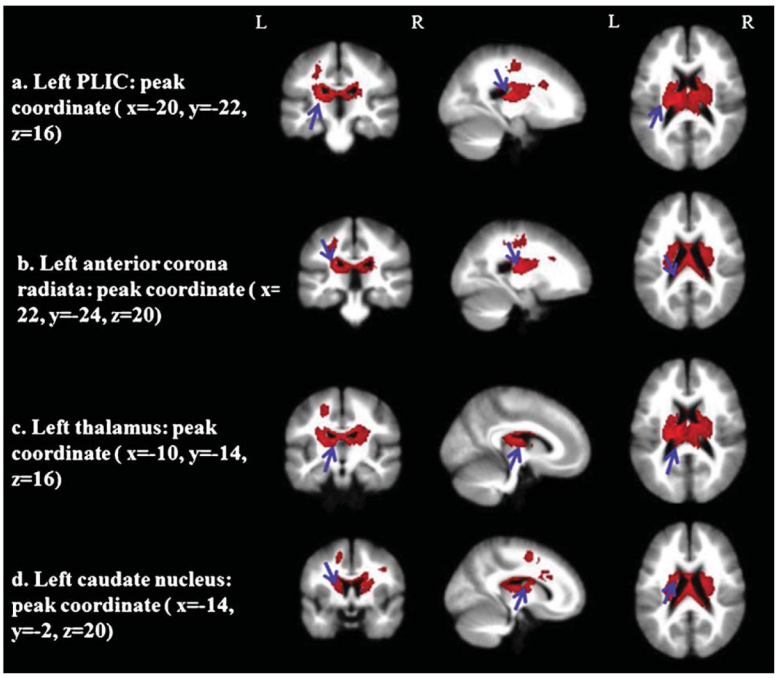

Fig. 3.

Regional FA decreases in AD compared with HC. Results ($p < 0.005$, correspond to SDM-Z ≤ -1.976) and a cluster size >10 voxels are reported. The (a–d) orderly showed the left PLIC, the left anterior corona radiata, the left thalamus and the left caudate nucleus. AD, Alzheimer's disease; FA, fractional anisotropy; HC, healthy control; L, left; PLIC, posterior limb of internal capsule; R, right.

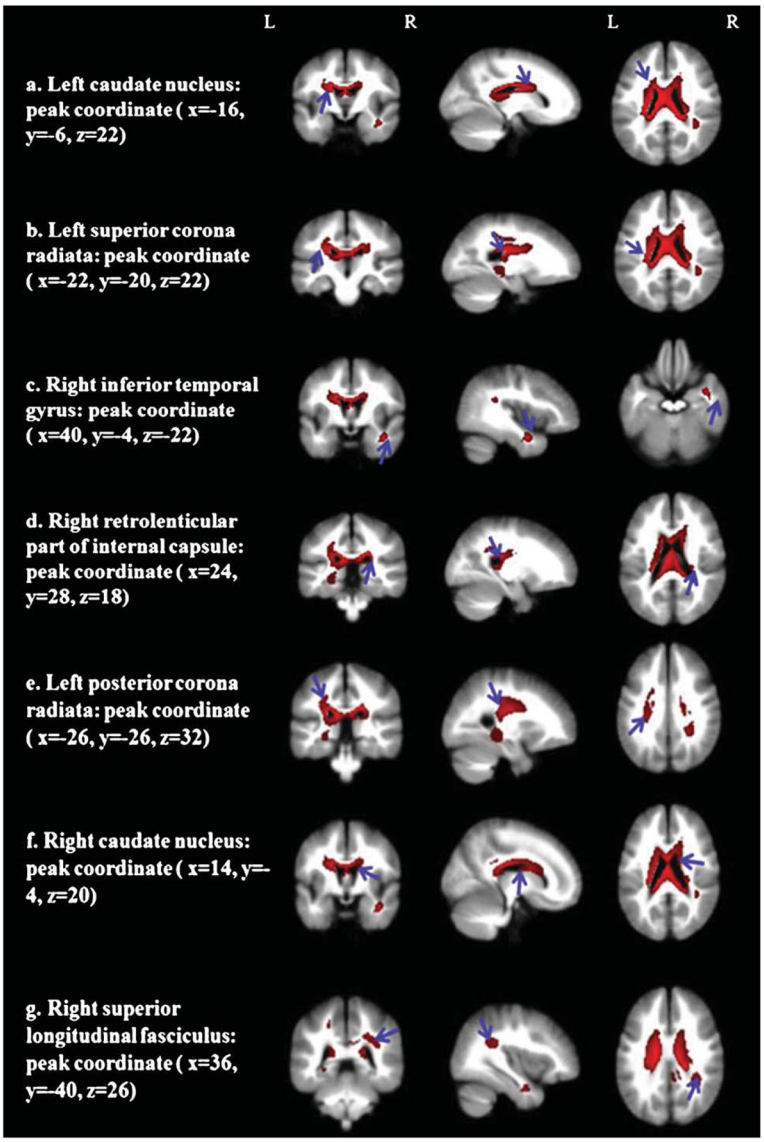

Fig. 4.

Regions with both WMV and FA reduction in AD compared with HC. Results ($p < 0.005$, correspond to SDM-Z ≤−1.976) and a cluster size >10 voxels are reported. The (a–g) successively indicate the left caudate nucleus, the left superior corona radiata and right inferior temporal gyrus, right retrolenticular part of internal capsule, left posterior corona radiate, right caudate nucleus, and right superior longitudinal fasciculus. AD, Alzheimer's disease; FA, fractional anisotropy; HC, healthy control; L, left; R, right; WMV, white matter volume.

Table 1

Demographic characteristics of the 16 data sets included in the meta-analysis

Studies	AD					HC			
	Number (female)	Age (mean)	Years of education (mean)	MMSE (mean)	Main diagnostic criteria	Number (female)	Age (mean)	Years of education (mean)	MMSE (mean)
White matter volume									
Baxter et al. [23]	15 (4)	75.5	14.7	—	DSM-IV criteria for dementia; NINCDS-ADRDA: probable AD	15 (8)	76.4	15.3	28.5
Canu et al. [24] (LOAD)	24 (16)	77.8	5.3	21.2	NINCDS-ADRDA: probable AD	24 (17)	76.4	9.6	28.3
Canu et al. [24] (EOAD)	18 (13)	62.5	7.7	20.1	NINCDS-ADRDA: probable AD	18 (13)	62.4	9.3	29.1
Canu et al. [25]	17 (14)	76.7	5.5	14.1	NINCDS-ADRDA: probable AD	13 (6)	72.6	9.2	28.9
Guo et al. [26]	13 (7)	72.1	—	18.5	NINCDS-ADRDA: probable AD	14 (8)	70.4	—	28.5
Honea et al. [27]	60 (37)	74.3	15.3	26.2	NINCDS-ADRDA: probable AD	56 (33)	73.3	16.4	29.4
Li et al. [28]	19 (9)	72.6	11.3	18.9	NINCDS-ADRDA: probable AD	20 (10)	70.7	10.9	29.5
Migliaccio et al. [29] (EOAD)	16 (6)	60.7	15.8	21.3	NINCDS-ADRDA: probable AD	72 (42)	62.3	17.6	29.8
Serra et al. [30]	9 (6)	72.4	9.9	18.2	NINCDS-ADRDA: probable AD	13 (4)	64.1	14.3	28.9
Takahashi et al. [31]	51 (31)	72.6	—	18.7	NINCDS-ADRDA: probable AD	40 (20)	72.0	—	29.6
Villain et al. [32]	18 (15)	69.5	—	24.3	—	15 (8)	66.5	—	—
Fractional anisotropy									
Canu et al. [25]	17 (14)	76.7	5.5	14.1	NINCDS-ADRDA: probable AD	13 (6)	72.6	9.2	28.9
Gao et al. [33]	18 (8)	76.47	4.86	20.07	NINCDS-ADRDA: probable AD	17 (8)	78.41	5.28	28.88
Medina et al. [34]	14 (9)	77.4	15.2	24.5	NINCDS-ADRDA: probable AD	21 (11)	77.3	5.1	29.3
Rose et al. [35]	13	76.8	—	22.3	NINCDS-ADRDA: probable AD	13	75.8	—	—
Zhang et al. [36]	18 (7)	62.8	—	21.7	NINCDS-ADRDA: probable AD	19 (8)	61.5	—	29.5

AD, Alzheimer's disease; DSM-IV, Diagnostic and Statistical Manual of Mental Disorders; EOAD, early onset AD; FA, fractional anisotropy; HC, health controls; LOAD, late onset AD; MMSE, Mini Mental State Examination; NINCDS-ADRDA, the National Institute of Neurological and Communicative Disorders and Stroke and the Alzheimer's Disease and Related Disorders Association; WMV, white matter volume.

Table 2

Technique details of VBM studies in current meta-analysis

Study	MRI scanner	Software	Smoothing (FWHM)	*p*-value	Coordinates
White matter volume					
Baxter et al. [23]	1.5T	SPM2	8 mm	$p < 0.0001$ (uncorrected)	6
Canu et al. [24] (LOAD)	1.0T	SPM8	8 mm	$p < 0.001$ (uncorrected)	14
Canu et al. [24] (EOAD)	1.0T	SPM8	8 mm	$p < 0.001$ (uncorrected)	15
Canu et al. [25]	3.0T	SPM5	8 mm	$p < 0.001$ (uncorrected)	37
Guo et al. [26]	3.0T	SPM2	8 mm	$p < 0.05$ (FDR corrected)	15
Honea et al. [27]	3.0T	SPM5	10 mm	$p < 0.001$ (FWE corrected)	6
Li et al. [28]	1.5T	SPM	8 mm	$p < 0.05$ (corrected)	3
Migliaccio et al. [29] (EOAD)	1.5T	SPM5	8 mm	$p < 0.0001$ (FWE corrected)	4
Serra et al. [30]	3.0T	SPM5	12 mm	$p < 0.05$ (corrected)	2
Takahashi et al. [31]	1.5T	SPM8	6 mm	$p < 0.001$ (uncorrected)	3
Villain et al. [32]	1.5T	SPM2	14.6 mm	$p < 0.05$ (uncorrected)	5
Fractional anisotropy					
Canu et al. [25]	3T	SPM5	8 mm	—	20
Gao et al. [33]	3T	SPM5	6 mm	$p < 0.001$ (uncorrected)	19
Medina et al. [34]	1.5T	SPM99	—	$p < 0.01$ (corrected)	14
Rose et al. [35]	1.5T	—	—	$p < 0.05$ (corrected)	3
Zhang et al. [36]	4T	SPM2	4 mm	$p < 0.05$ (FDR corrected)	11

AD, Alzheimer's disease; EOAD, early onset AD; FDR, false discovery rate; FWE, family-wise error; FWHM, full width at half-maximum; LOAD, late onset AD; SPM, Statistical Parametric Mapping; T, Tesla; VBM, voxel-based morphometry.

Table 3

Regions of significant reduction in WMV and FA between AD patients and HC

Region	MNI coordinates	SDM z-value	*p*-value	Number of voxels	Jackknife sensitivity analysis (combination of studies detecting the differences)
Decreased WMV					
Right inferior temporal gyrus	44, −8, −28	−3.033	0.52×10^{-4}	354	7 out of 11 (Canu et al. [24] (EOAD), Canu et al. [25], Migliaccio et al. [29] (EOAD), Takahashi et al. [31])
Splenium of corpus callosum	12, −38, 22	−2.952	0.59×10^{-4}	913	11 out of 11
Right parahippocampal gyrus	34, −26, −16	−2.806	0.98×10^{-4}	154	11 out of 11
Right hippocampus	26, −38, 2	−2.519	3.85×10^{-4}	193	9 out of 11 (Guo et al [26], Takahashi et al. [31])
Left inferior temporal gyrus	−44, −6, −30	−2.454	5.15×10^{-4}	162	11 out of 11
Decreased FA					
Left PLIC	−20, −22, 16	−2.934	0.65×10^{-5}	420	1 out of 5 (only Zhang et al. [36])
Left anterior corona radiata	−22, −24, 20	−2.881	0.13×10^{-4}	40	2 out of 5 (only Medina et al. [34], Rose et al. [35])
Left thalamus	−10, −14, 16	−2.749	0.13×10^{-4}	270	4 out of 5 (Gao et al. [33])
Left caudate nucleus	−14, −2, 20	−2.723	0.13×10^{-4}	90	5 out of 5
Multimodal analysis: Decreased WMV and FA					
Left caudate nucleus	−16, −6, 22	—	0.69×10^{-6}	120	—
Left superior corona radiata	−22, −20, 22	—	0.16×10^{-5}	451	—
Right inferior temporal gyrus	40, −4, −22	—	0.15×10^{-4}	109	—

FA, fractional anisotropy; HC, health controls; MNI, Montreal Neurological Institute; PLIC, posterior limb of internal capsule; WMV, white matter volume.

Table 4

The meta-regression results of regional WMV

Region	MNI coordinates	SDM z-value	*p*-value	Number of voxels
Differences between patients with maximum MMSE and HC				
Left parahippocampal gyrus	−28, −24, −26	−4.799	6.52×10^{-6}	155
Left inferior temporal gyrus	−44, −16, −24	−3.889	3.72×10^{-4}	215
Right parahippocampal gyrus	32, −24, −26	−3.820	4.89×10^{-4}	123
Differences between patients with minimum MMSE and HC				
Right hippocampus	38, −34, −10	−3.496	6.52×10^{-6}	528
Left inferior temporal gyrus	−52, −46, −12	−2.426	2.04×10^{-3}	27
Splenium of corpus callosum	−10, −42, 10	−2.347	2.78×10^{-3}	19

HC, health controls; MNI, Montreal Neurological Institute; MMSE, the Mini-Mental State Examination; WMV, white matter volume.